SUPPLEMENTARY FIGURE LEGENDS

Sup. Fig. 1. ER retention of ATP7B^{H1069Q} mutant does not require activation of MEK/ERK signaling pathway.

(A) HepG2 cells were infected with Ad-ATP7B^{WT}-GFP or Ad-ATP7B^{H1069Q}-GFP and prepared western blot to reveal levels of phosphorylated and total ERK (p-ERK and ERK respectively). Both p-ERK and ERK levels did not exhibit significant changes in cells expressing ATP7B^{H1069Q} mutant. **(B)** HepG2 cells were infected withAd-ATP7B^{H1069Q}-GFP and incubated for 2h with BCS. Specific inhibitors of MEK/ERK, PD318088 (5μM) or GSK1120212 (5μM), were added to the cells 24h before fixation (as indicated in corresponding panels). Fixed cells were than labeled for TGN46 and visualized under confocal microscope. Treatment with each inhibitor did not recover ATP7B^{H1069Q} from the ER to the TGN. Scale bar: 5μm (B).

Sup. Fig. 2. Characterization of the impact of p38 and JNK inhibitors on trafficking of ATP7B and its mutant.

(A) Hela cells were infected with Ad-ATP7B^{WT}-GFP incubated overnight exposure to 200 μM BCS and fixed or incubated for additional 2h with 100 μM $CuSO_4$ (as indicated on panels). ATP7B^{WT} moves from the Golgi (arrowheads) to PM and vesicles (arrows) in response to $CuSO_4$. p38 inhibitor SB202190 (5μM) or JNK inhibitor SP600125 (2μM) were added to the cells 24h before fixation (as indicated in corresponding panels). Both inhibitors did not affect ability of ATP7B^{WT} to traffic from the Golgi to PM and vesicles (arrows in bottom row) in response to increased Cu. **(B)** Hela cells were infected with Ad-ATP7B^{H1069Q}-GFP fo 2h with 100 μM $CuSO_4$ (as indicated on panels). p38 inhibitor SB202190 or JNK inhibitor SP600125 were added to the cells 24h before fixation at different concentrations. Then the cells were stained for TGN46 and analyzed under confocal microscope. Percentage of the cells (average ± SD, n=10 fields) with ATP7B signal in the ER was calculated. Both p38 and JNK inhibitors reduced percentage of the

cells that exhibit ATP7B^{H1069Q} in the ER in concentration-dependent manner. Scale bar: 5 μm (A).

Sup. Fig. 3. p38 inhibitor, JNK inhibitor or their mixture correct ATP7B^{H1069Q} localization with similar strength.

(A) HeLa cells were infected with Ad-ATP7B^{WT}-GFP or Ad-ATP7B^{H1069Q}-GFP, incubated for 2h with 200 μM BCS and fixed. p38 inhibitor SB202190 (5μM) or JNK inhibitor SP600125 (2μM) or mixture of both inhibitors were added to the cells 24h before fixation (as indicated in corresponding panels). Fixed cells were than labeled for TGN46 and visualized under confocal microscope. p38 and JNK inhibitors as well as their mixture corrected ATP7B^{H1069Q} from the ER to the Golgi with similar amplitude. **(B)** Fluorescence of ATP7B signal in the Golgi (average ± SD, n=40 cells) was quantified and normalized to total cell fluorescence. p38 and JNK inhibitors (or their mixture) caused increase of ATP7B^{H1069Q} signal in the Golgi region. Exposure of the cells to the mixture of inhibitors does not significantly increase ATP7B^{H1069Q} signal in the Golgi when compared to each inhibitor alone. **(C)** The percentage of the cells (average ± SD, n=10 fields) with an ATP7B signal in the ER, or Golgi was calculated. p38 and JNK inhibitors alone as well as their combination reduced the percentage of the cells exhibiting ATP7B^{H1069Q} in the ER and increases the number of cells in which the mutant was corrected to the Golgi. Single inhibitors and their mixture exhibit similar strength in correction of ATP7B^{H1069Q} intracellular phenotype. ✻✻✻- $p<0.001$; ✻✻- $p<0.01$; ✻- $p<0.05$; ns – $p>0.05$ (t-test). Scale bar: 5 μm (A).

Sup. Fig. 4. Acute treatment with p38 or JNK inhibitor does not rescue ATP7B^{H1069Q} mutant from the ER.

(A) HeLa cells were infected with Ad-ATP7B^{H1069Q}-GFP and incubated for 2h with 100 μM $CuSO_4$. p38 inhibitor or JNK inhibitor were added to the cells 1h before fixation (as indicated in corresponding panels). Fixed cells were than labeled for TGN46 and visualized under confocal microscope. Short-term treatment with either p38 orJNK inhibitor did not recover ATP7B^{H1069Q} from the ER. **(B)** Percentage of the cells (average ± SD, n=10 fields) with ATP7B signal in the ER, was calculated. Both p38 and JNK

inhibitors did not reduce percentage of the cells that exhibit ATP7B^{H1069Q} in the ER after 1h treatment. Scale bar: 5 μm (A).

Sup. Fig. 5. p38 and JNK inhibitors increase ATP7B^{H1069Q} amounts in plasma membrane subcellular fraction.

(A) HepG2 cells were infected with Ad-ATP7B^{WT}-GFP and incubated for 2h with 100 μM $CuSO_4$. The cells were then subjected to subcellular fractionation (see Methods) and isolated membrane fractions labeled with different markers. Western blot indicates that ATP7B^{WT} was enriched in fractions #5 and #10. However, fractions #2-5 were cross-contaminated with ER (PDI), Golgi (GM130) and at some extent with plasma membrane (Na/K-ATPase) indicating poor separation between corresponding organelles. In contrast, fraction #10 contained only Na/K-ATPase demonstrating significant enrichment in plasma membranes (PMs). Therefore, Na/K-ATPase positive PM fractions were used further for evaluation of ATP7B^{WT} or ATP7B^{H1069Q} delivery to the cell surface. **(B)** HepG2 cells were infected with Ad-ATP7B^{WT}-GFP or Ad-ATP7B^{H1069Q}-GFP and treated with $CuSO_4$ and subjected to fractionation as in panel A. p38 inhibitor or JNK inhibitor were added to the cells 24h before fractionation procedure. Light PM fractions (#10-12) were prepared for Western blot and labeled with antibodies against GFP and against Na/K-ATPase. Na/K-ATPase-positive PM fractions from the p38 inhibitor- or JNK inhibitor-treated cells exhibit higher amounts of ATP7B^{H1069Q} then the same fractions from untreated cells indicating that both inhibitors facilitate ATP7B^{H1069Q} delivery to the cell surface. **(C)** ATP7B signal in fractions #10 (shown in panel B) was quantified using ImageJ software and normalized for Na/K-ATPase signal in corresponding lanes. Plot shows that both p38 and JNK inhibitors increase quantities of ATP7B^{H1069Q} associated with PM fractions.

Sup. Fig. 6. Suppression of p38 and JNK allows ATP7B^{H1069Q} to reach canalicular surface of polarized HepG2 cells.

HepG2 cells were grown at the conditions that allow their full polarization (see Methods). Then the cells were infected with Ad-ATP7B^{WT}-GFP (A) or Ad-ATP7B^{H1069Q}-GFP (B-D) and incubated for 4h with 100 μM $CuSO_4$. p38 (C) or JNK (D) inhibitors were added

to the cells 24h before fixation. Fixed cells were labeled for canalicular marker MRP2 and visualized under confocal microscope. Cu induces delivery of $ATP7B^{WT}$ to the canalicular domain (A, arrows) while the mutant remains retained within the ER and does not reach the canalicular srface (B, arrows). Both p38 and JNK inhibitors allows $ATP7B^{H1069Q}$ to de delivered to the canalicular domain (C, D; arrows) in polarized HepG2 cells. Scale bar: 4 μm (A-D).

Sup. Fig. 7. Inhibitors of p38 and JNK reduce copper levels in cells expressing $ATP7B^{H1069Q}$ mutant.

HepG2 cells were infected with Ad-$ATP7B^{WT}$-GFP (A) or Ad-$ATP7B^{H1069Q}$-GFP (B-D), incubated for 2h with 100 μM $CuSO_4$ and loaded with CS3 before fixation. p38 (C) or JNK (D) inhibitors was added to the cells 24h before fixation. **(A, B)** Cells expressing $ATP7B^{H1069Q}$ exhibit higher CS3 signal (and hence Cu levels) than cells expressing $ATP7B^{WT}$. Arrows in B indicate $ATP7B^{H1069Q}$ –negative cells, which display CS3 levels similar to those detected in the neighbor cell expressing the mutant. This indicates that expression of mutant does not allow cells to efflux Cu efficiently. **(C, D)** Both p38 and JNK inhibitors decrease CS3 fluorescence in $ATP7B^{H1069Q}$-expressing cells. Arrows in C and D show higher CS3 levels in cells expressing lower $ATP7B^{H1069Q}$ amounts, indicating that capacity of p38/JNK-inhibitor treated cells to eliminate Cu correlates to amount of the expressed mutant. Scale bar: 10 μm (A-D).

Sup. Fig. 8. Inhibitors of p38 and JNK do not impact trafficking of VSVG.

(A) HeLa cells were transfected with DNA encoding temperature-sensitive version of VSVG-GFP, incubated overnight at 40°C to block the newly-synthetized protein in the ER and fixed directly (left column) or incubated at 32°C for additional time periods (to activate VSVG-GFP trafficking) as indicated in panels. p38 inhibitor (mid row) or JNK inhibitor (bottom row) were added to the cells 24h before fixation. Fixed cells were than analyzed using confocal microscopy. Both p38 and JNK inhibitors did not affect VSVG delivery from the ER to the Golgi (arrowheads) and further to the PM (arrows). **(B)** Percentage of the cells (average ± SD, n=10 fields) with ATP7B signal in the ER, Golgi or PM was calculated. Cells exhibit similar dynamics of VSVG progression through the

secretory pathway in control cells and in cells treated with p38 or JNK inhibitor. Scale bar: 5.2 μm (A).

Sup. Fig. 9. p38 and JNK inhibitors does not affect interaction of ATP7B^{H1069Q} with COMMD1.

(A) HepG2 cells expressing COMMD1-GST were infected with Ad-ATP7B^{WT}-GFP or Ad-ATP7B^{H1069Q}-GFP, incubated for 2h with 100 μM $CuSO_4$ and lysed. ATP7B^{WT} and ATP7B^{H1069Q} we pulled down from lysates using anti-GFP antibody. Both immuno-precipitates (IPs) and total cell lysates were subjected to Western blot to reveal ATP7B and COMMD1. Western blot shows higher levels of COMMD1 in ATP7B^{H1069Q} IP, indicating enhanced interaction of the mutant with COMMD1. **(B)** HepG2 cells expressing COMMD1-GST were infected with Ad-ATP7B^{H1069Q}-GFP, treated with Cu and prepared for IP and Western blot as described in panel A. p38 or JNK inhibitor was added to the cells 24h before they were lysed. Neither inhibitor reduced COMMD1 binding to ATP7B^{H1069Q}, indicating that this interaction is unlikely to be involved in mutant correction by p38 or JNK inhibitors.

Fig. S1. Chesi et al.

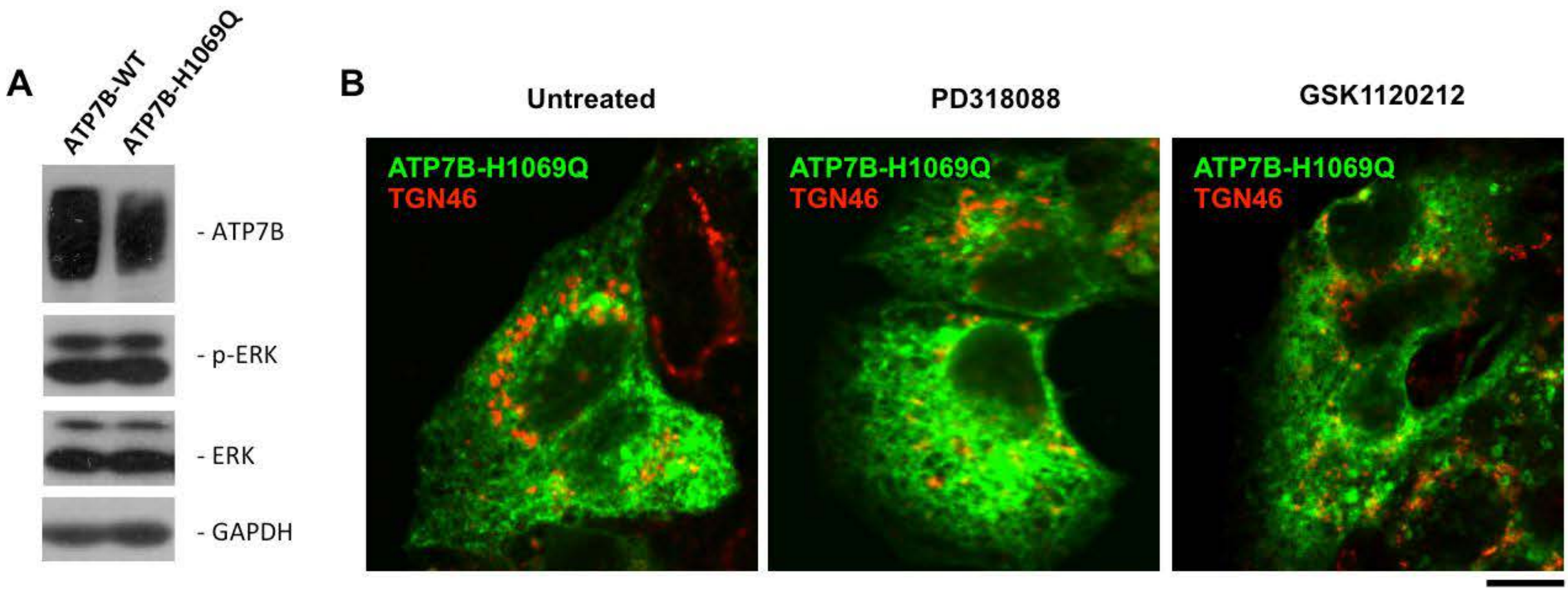

Fig. S2. Chesi et al.

A

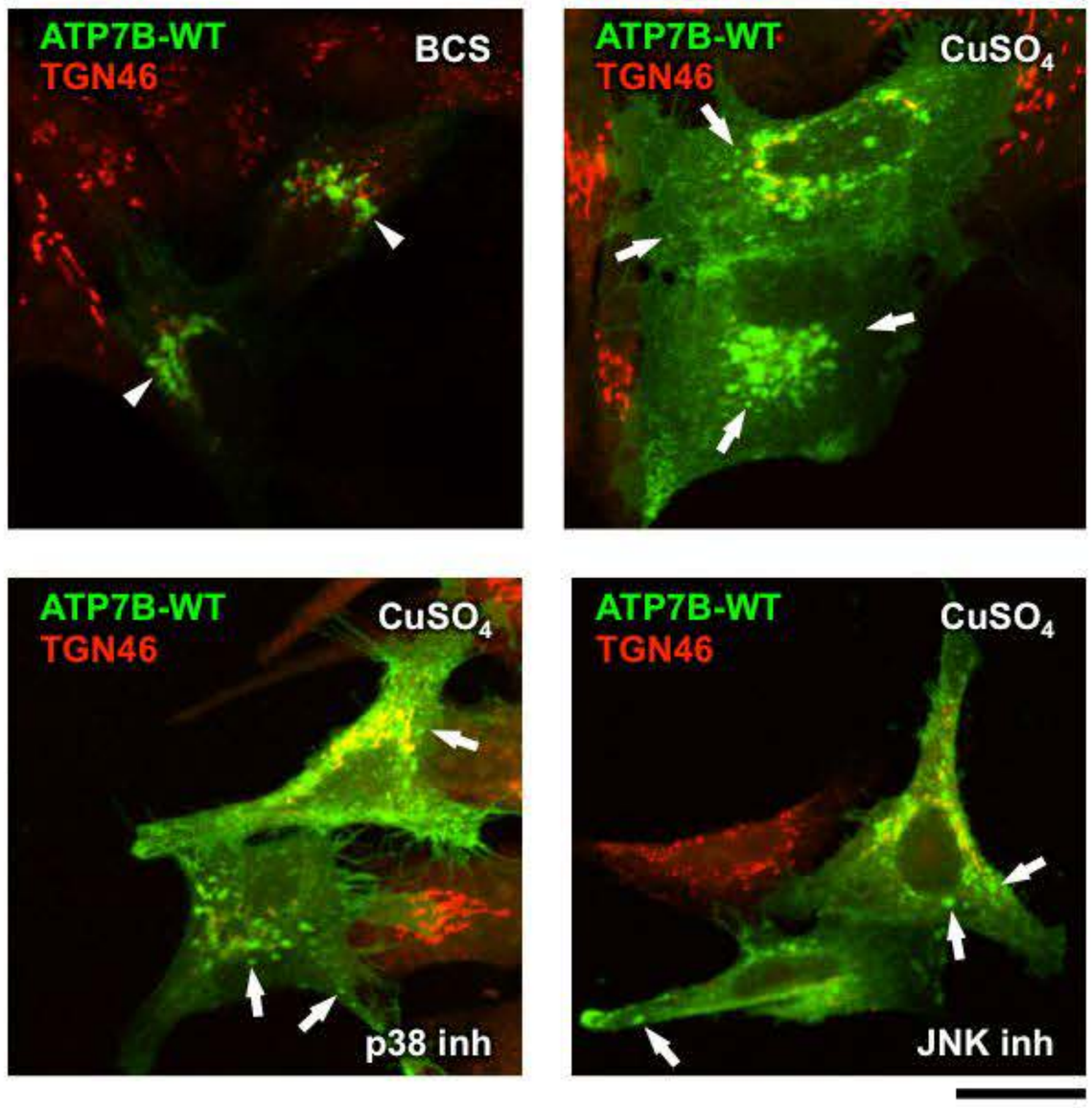

B

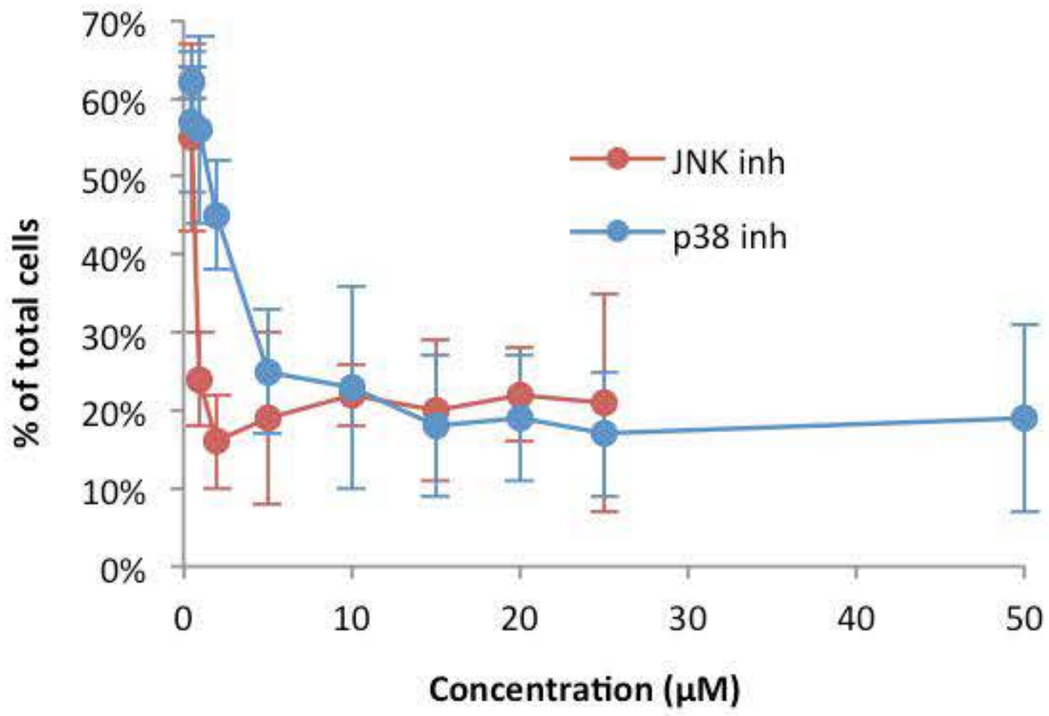

Fig. S3. Chesi et al.

A

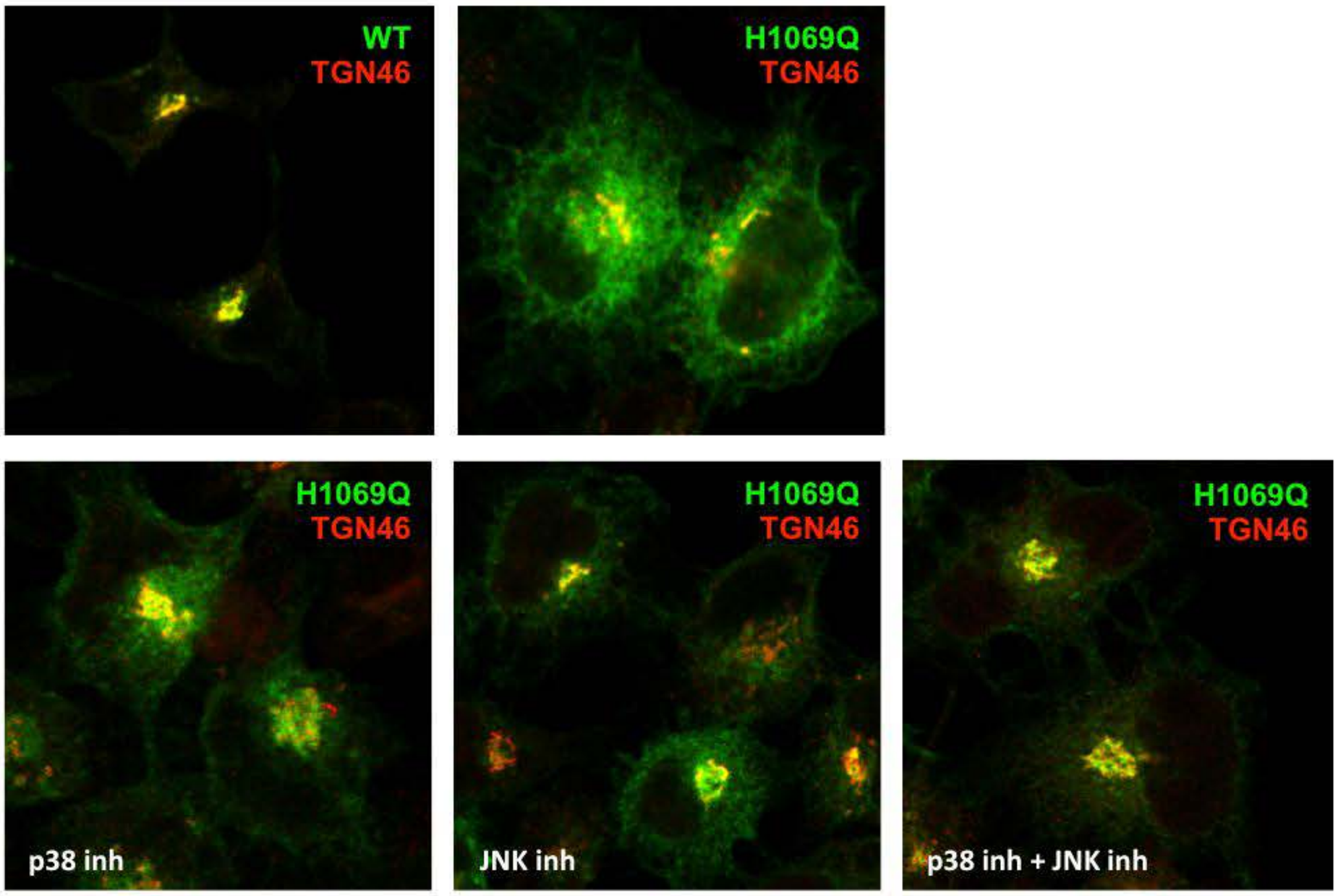

B

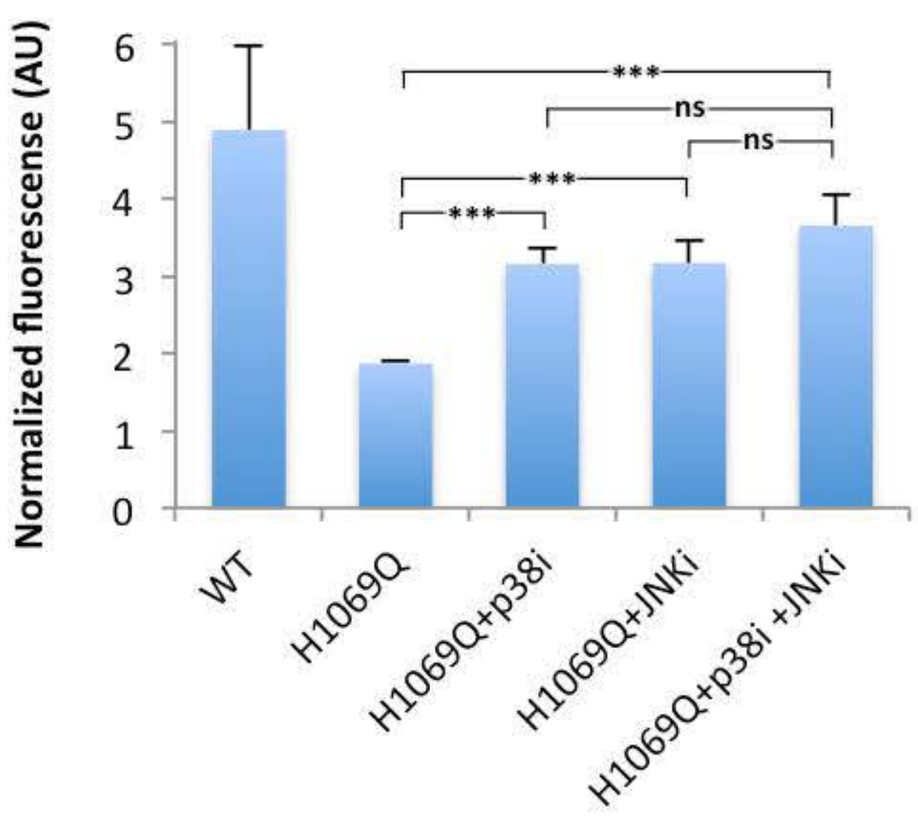

C

Fig. S4. Chesi et al.

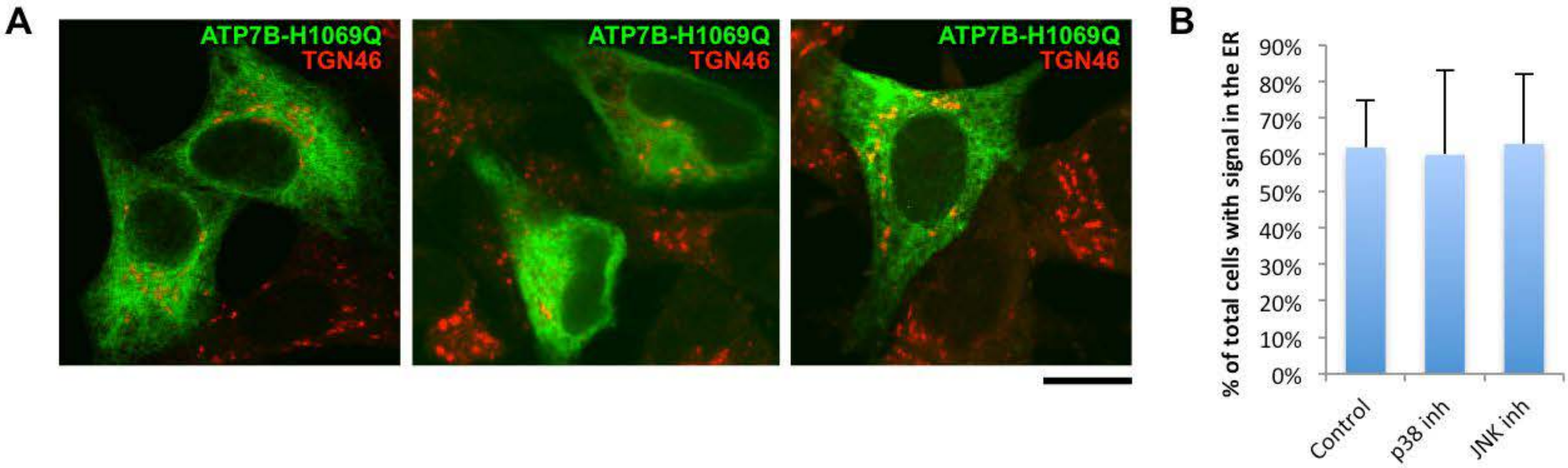

Fig. S5. Chesi et al.

A

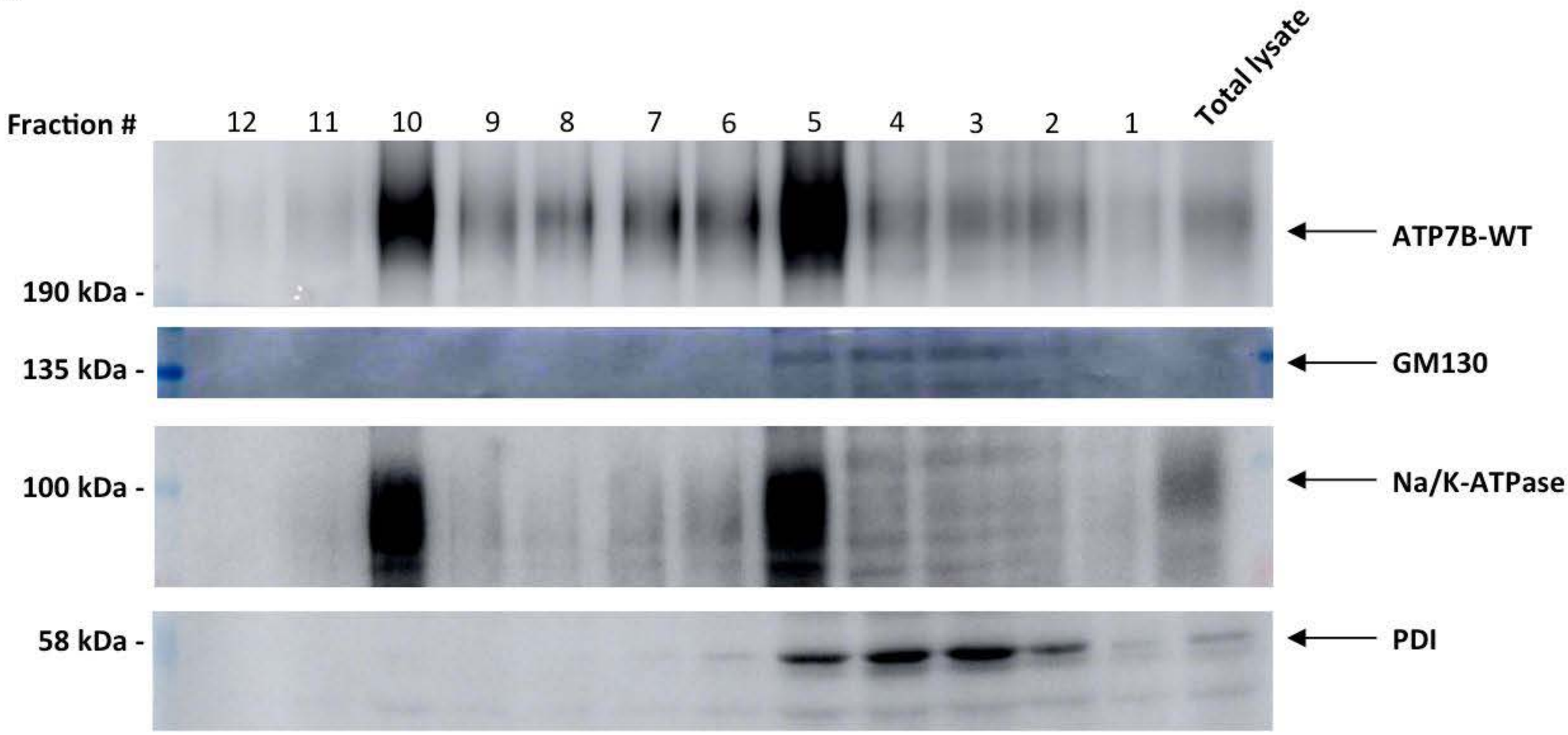

B

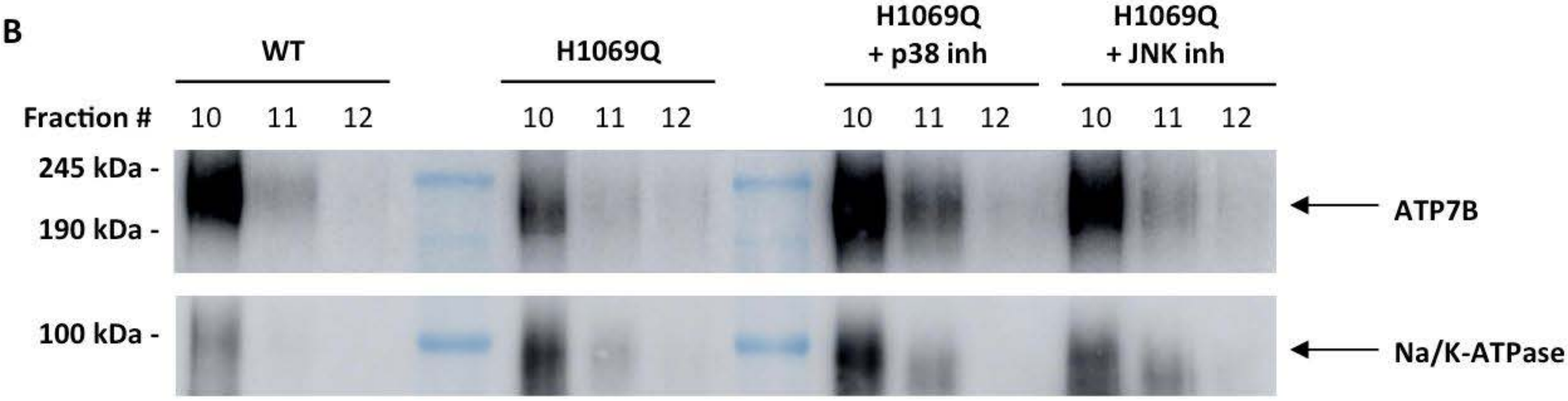

C

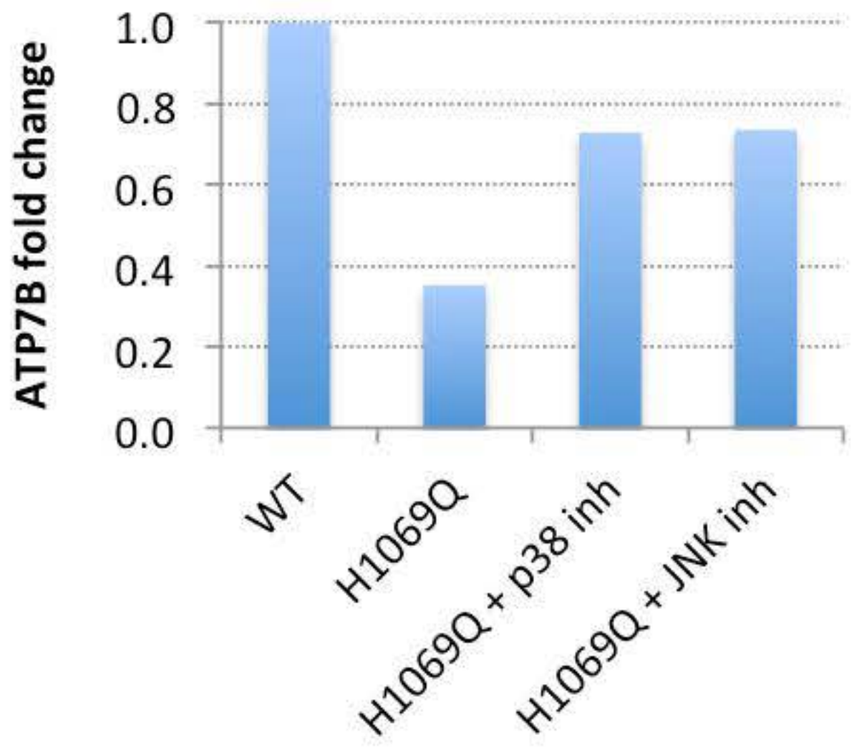

Fig. S6. Chesi et al.

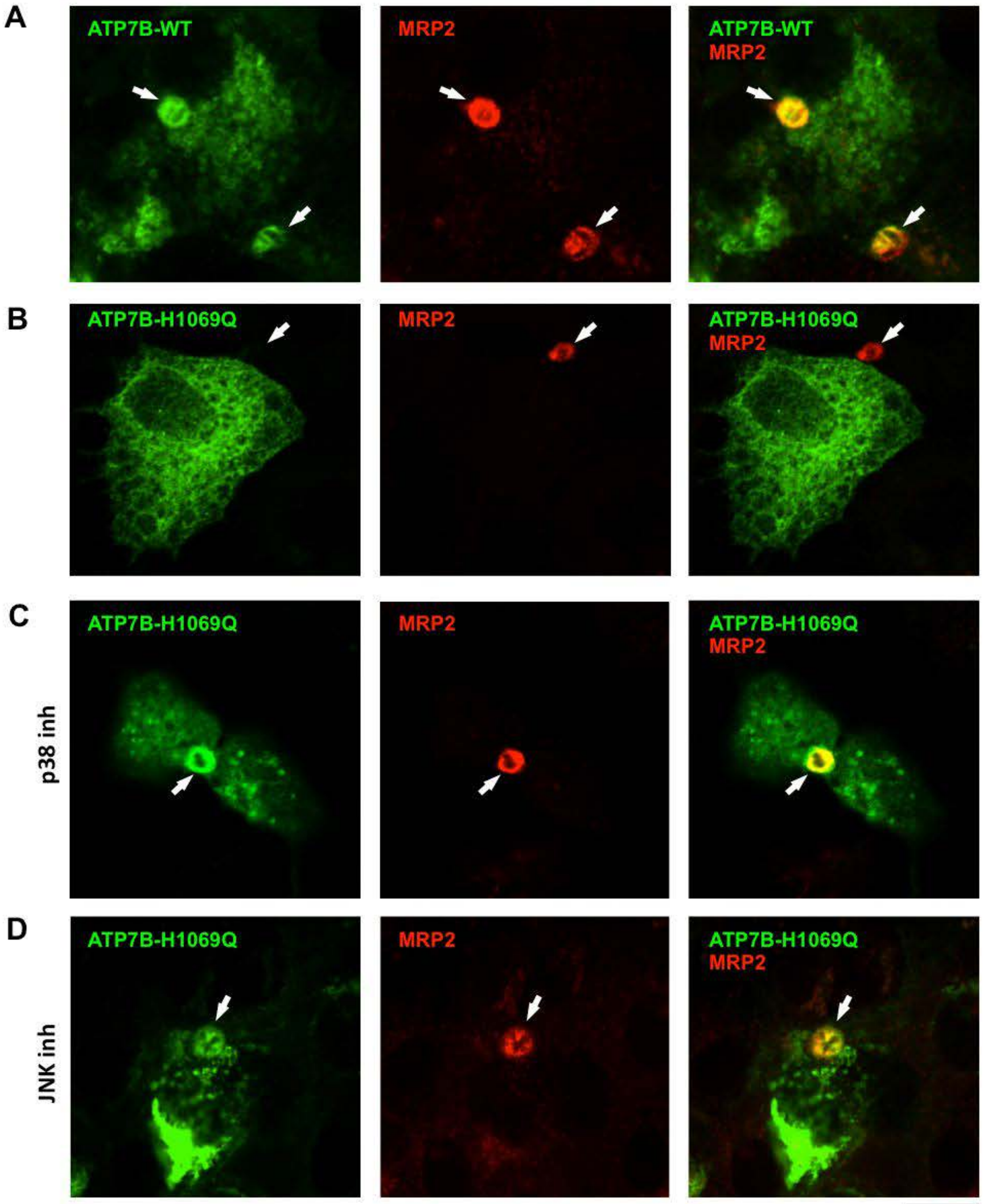

Fig. S7. Chesi et al.

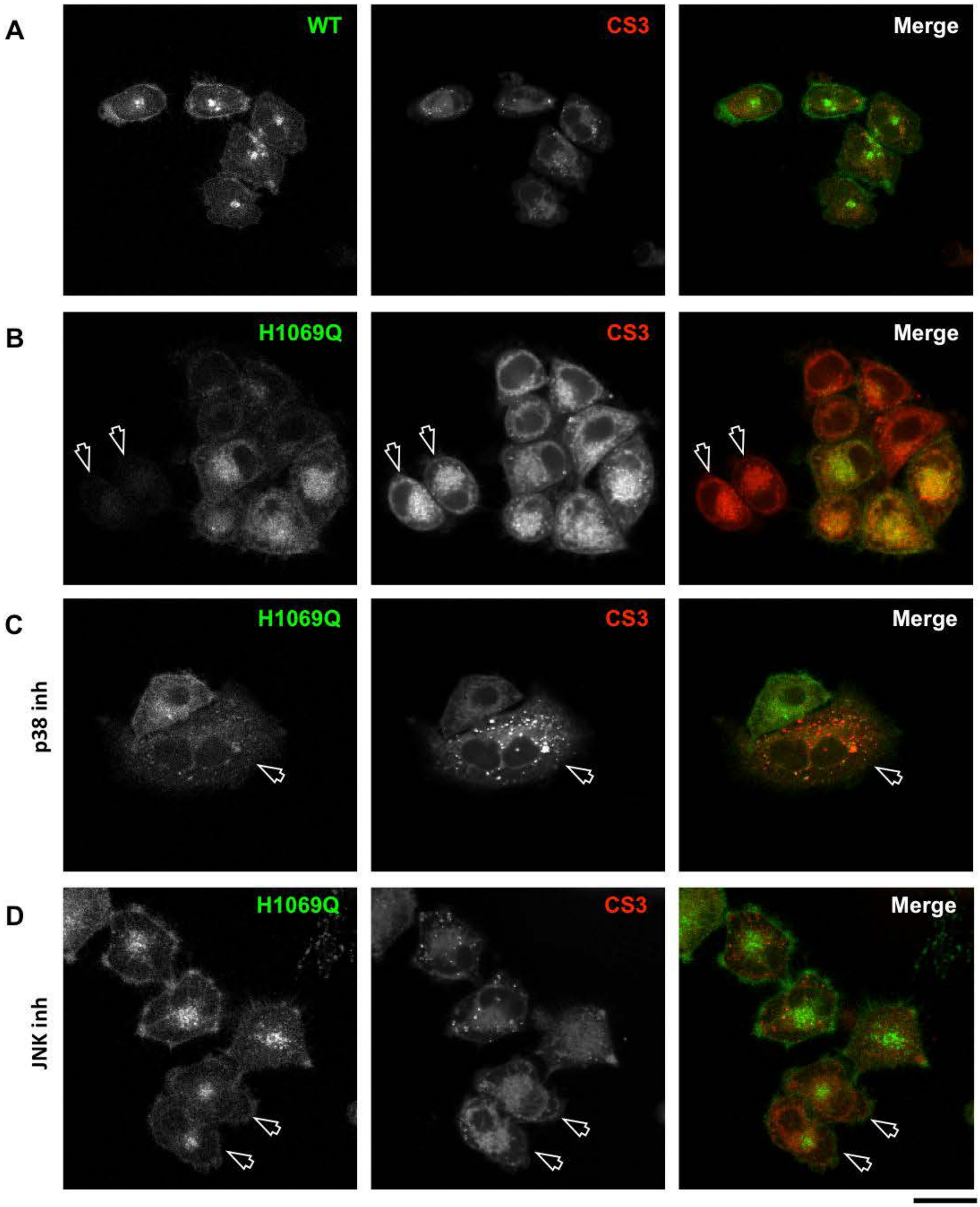

Fig. S8. Chesi et al.

A

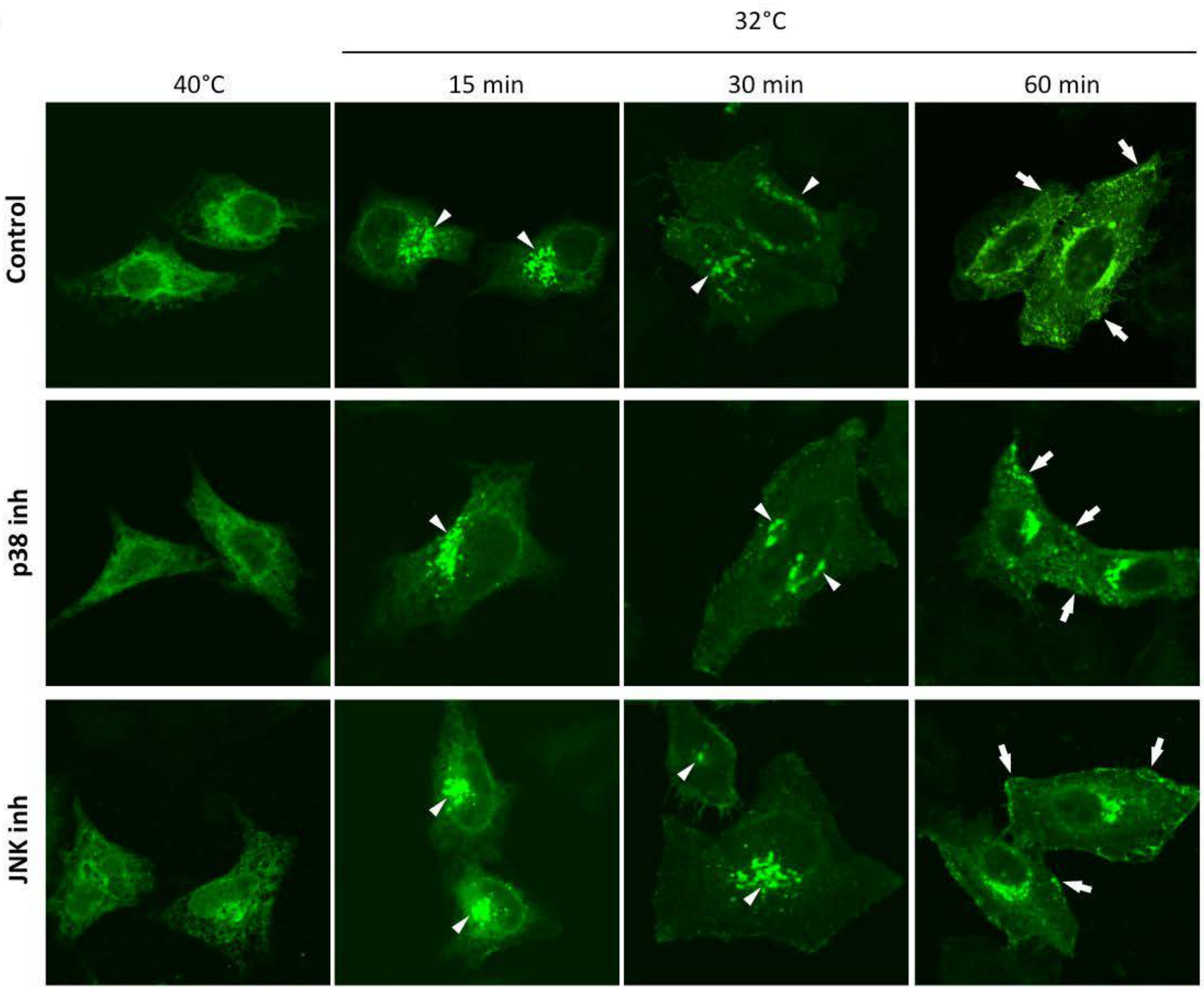

B

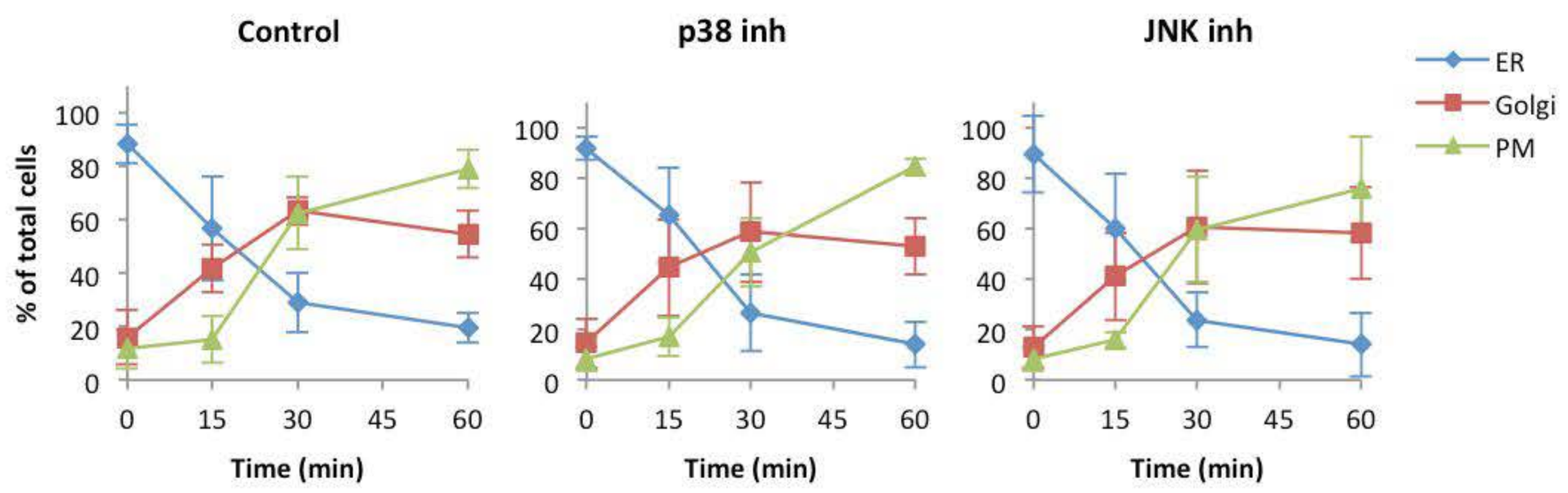

SUPPLEMENTARY TABLE 1.
Gene ontology (GO) categories of genes differentially expressed in ATP7B-H1069Q expressing cells versus ATP7B-WT expressing cells.

Gene Ontology (GO) Categories	Gene Ontology (GO) ID	Number of differentially expressed Genes with this GO category	Name of differentially expressed Genes with this GO category	Population Hits (PH)	Population Total (PT)	Fold Enrichment (FE)	False Discovery Rate (FDR)
regulation of apoptosis	GO:0042981	41	CADM1, MCL1, CLU, TAF9B, SOX4, CDH1, CHEK2, SFN, PTEN, MAGED1, TDGF3, NOD2, TP53I3, CDKN2A, SQSTM1, CDKN2C, CDKN2D, AGT, TDGF1, PYCARD, FAIM, CAT, FAS, FOSL1, HELLS, MAP2K6, KNG1, TXNIP, DEPDC6, MSH6, LGALS1, ITGA1, SKP2, BIRC3, CDK5, SOD2, BNIP3L, AVEN, ID3, TNFAIP3, IGFBP3, IFI6	804	13528	2,41210034	5,78E-04
regulation of cell proliferation	GO:0042127	35	FGFR2, BLM, IFITM1, IL18, CLU, IFI30, SOX4, SFN, PTEN, TIMP1, TRIB1, MAGED1, CD47, WARS, TDGF3, CD9, CDKN2A, CDKN2C, CDKN2D, AGT, TDGF1, SERPINE1, FOSL1, TXNIP, STS, TESC, IL8, EGR4, SPARC, CDKN3, SOD2, CORO1A, CBLB, EREG, BTG3, IGFBP3	787	13528	2,10358891	0,092770639
response to drug	GO:0042493	15	TXNIP, NAT8B, NAT8, MFSD9, MAT2A, CDH1, PTEN, SOD2, SERPINA7, CA9, ENO3, GNAS, LOX, FOSL1, PDZK1, MAP2K6	216	13528	3,28477078	0,341239702
regulation of cell cycle	GO:0051726	19	BLM, NEK2, SKP2, NUSAP1, ANAPC10, CHEK2, SFN, OBFC2A, CDKN3, CDK5, PTEN, CDT1, CDKN2A, EREG, CDKN2C, CDKN2D, BTG3, ID3, FOSL1	331	13528	2,71514588	0,404894167
regulation of cellular component size	GO:0032535	16	FGFR2, DEPDC6, TAF9B, SFN, CSRP2, N6AMT1, LEFTY1, CORO1A, CDKN2A, NDRG4, CDKN2C, MAPT, CDKN2D, AGT, TMSB4X, TMSL3	271	13528	2,79266121	1,099341419
oxidation reduction	GO:0055114	27	CYP24A1, SORD, PYROXD1, IFI30, GLDC, GPX2, TP53I3, P4HA2, P4HA1, PLOD2, IDH2, HSD17B6, BDH2, LOX, CAT, HADH, GPD1, NOX3, MTHFD2L, SOD2, OGFOD1, G6PD, BLVRB, PCYOX1, DIO1, GLYR1, AOC3	639	13528	1,9986211	1,758146094
positive regulation of immune system process	GO:0002684	14	MICB, BLM, CADM1, IL18, F2RL1, CLU, AQP3, CD47, CBLB, NOD2, CORO1A, EREG, SPG21, CFD	238	13528	2,78239408	2,783907866
DNA replication	GO:0006260	12	POLD3, PRIM1, GINS2, RFC4, BLM, POLE2, DTL, MRE11A, CDKN2D, MCM10, CHAF1A, CDT1	190	13528	2,98741259	3,954136316
response to DNA damage stimulus	GO:0006974	18	EXO1, MSH6, NUDT1, BLM, DTL, MRE11A, SFN, CHEK2, OBFC2A, ATMIN, SOD2, POLD3, RFC4, POLE2, FANCI, CDKN2D, CHAF1A, MAP2K6	373	13528	2,28260747	4,081799187
regulation of cell adhesion	GO:0030155	10	KNG1, CD47, TDGF3, TESC, CDKN2A, IL8, IL18, TDGF1, SERPINI1, PTEN, DPP4	137	13528	3,45260579	4,180275525

Gene ontology descriptions of biological processes were assigned on the basis of the informations retrieved from DAVID (http://david.abcc.ncifcrf.gov/), considering a False Discovery Rate (FDR) less than 5; Population Hits (PH) corresponds to the number of genes of each GO category on the whole background list; Population Total (PT) corresponds to the total number of genes on the whole background list; Fold Enrichment (FE) estimates the enrichment degree of the corresponding GO category

SUPPLEMENTARY TABLE 2. List of ATP7B-WT-specific interactors.

Protein	CODE SP	GENE NAME	# Peptides	MW [kDa]	
Transferrin receptor protein 1	**P02786**	**TFRC**	**4**	**85**	
Peptide Sequences	Modifications	IonScore	Charge	MH+ [Da]	ΔM [ppm]
LAVDEEENADNNTK		53	2	1561.73	22.5
LLNENSYVPR		18	2	1204.81	250
SSGLPNIPVQTISR		28	2	1468.97	96
VEYHFLSPYVSPK		15	3	1566.08	183
Guanine nucleotide-binding protein subunit beta-2-like 1	**P63244**	**GNB2L1**	**11**	**35**	
Peptide Sequences	Modifications	IonScore	Charge	MH+ [Da]	ΔM [ppm]
IIVDELKQEVISTSSK		79	2	1789.27	155
VWQVTIGTR		47	2	1059.69	92.7
LWDLTTGTTTR		46	2	1264.85	158
YWLCAATGPSIK		46	2	1366.93	183
LWDLTTGTTTRR		36	3	1421.03	198
DETNYGIPQR		36	2	1192.63	61.6
LTRDETNYGIPQR		33	3	1562.96	111
VWNLANCK		32	2	1004.63	134
FSPNSSNPIIVSCGWDK		45	2	1907.94	29.9
IWDLEGK		26	2	860.61	188
60S ribosomal protein L7	**P18124**	**RPL7**	**8**	**29**	
Peptide Sequences	Modifications	IonScore	Charge	MH+ [Da]	ΔM [ppm]
IVEPYIAWGYPNLK		81	2	1663.17	123
IALTDNALIAR		71	2	1170.81	195
SVNELIYKR		38	2	1121.69	54.8
ASINMLR		35	2	804.51	91
EVPAVPETLK		34	2	1082.65	40.3
QIFNGTFVK		33	2	1053.77	190
SVNELIYK		32	2	965.63	106
AGNFYVPAEPK		30	2	1192.75	128
ADP/ATP translocase 3	**P12236**	**SLC25A6**	**7**	**33**	
Peptide Sequences	Modifications	IonScore	Charge	MH+ [Da]	ΔM [ppm]
DFLAGGIAAAISK		99	2	1233.89	170
YFPTQALNFAFK		54	2	1446.97	160
LLLQVQHASK		39	2	1136.79	100
GNLANVIR		38	2	856.53	38.4
GAWSNVLR		35	2	902.61	75.9
AAYFGVYDTAK		32	2	1205.73	124
EQGVLSFWR		26	2	1121.81	178
Vesicle-associated membrane protein-associated protein B/C	**O95292**	**VAPB**	**3**	**27**	
Peptide Sequences	Modifications	IonScore	Charge	MH+ [Da]	ΔM [ppm]
GPFTDVVTTNLK		66	2	1291.81	95.7
TVQSNSPISALAPTGK		51	2	1570.79	5.87
FRGPFTDVVTTNLK		15	3	1595.24	243
Glutathione S-transferase omega-1	**P78417**	**GSTO1**	**6**	**27**	
Peptide Sequences	Modifications	IonScore	Charge	MH+ [Da]	ΔM [ppm]
VPSLVGSFIR		51	2	1074.73	151
HEVININLK		46	2	1079.71	85.3
GSAPPGPVPEGSIR		32	2	1320.79	77.4
LLPDDPYEK		31	2	1089.65	135
FCPFAER		17	2	925.56	166
EFTKLEEVLTNK		17	3	1450.88	73.6
Ribonucleoside-diphosphate reductase subunit M2	**P31350**	**RRM2**	**2**	**51**	
Peptide Sequences	Modifications	IonScore	Charge	MH+ [Da]	ΔM [ppm]
FSQEVQITEAR		67	2	1307.61	-35.41
IEQEFLTEALPVK		58	2	1516.95	83.8
14-3-3 protein eta	**Q04917**	**YWHAH**	**2**	**28**	
Peptide Sequences	Modifications	IonScore	Charge	MH+ [Da]	ΔM [ppm]
AVTELNEPLSNEDR		82	2	1586.85	54.9
NSVVEASEAAYK		58	2	1267.65	28.6
LIM domain only protein 7	**Q8WWI1**	**LMO7**	**4**	**158**	
Peptide Sequences	Modifications	IonScore	Charge	MH+ [Da]	ΔM [ppm]
TSTTGVATTQSPTPR		74	2	1504.79	21.6
ISINQTPGK		45	2	957.61	79.8
WIDATSGIYNSEK		38	2	1484.33	422
RGESLDNLDSPR		35	3	1358.96	221
ATP-dependent Clp protease ATP-binding subunit clpX-like, mit	**O76031**	**CLPX**	**5**	**58**	
Peptide Sequences	Modifications	IonScore	Charge	MH+ [Da]	ΔM [ppm]
DVGGEGVQQGLLK		68	2	1299.67	-13.55
LLEGTIVNVPEK		47	2	1312.03	214
LLQDANYNVEK		32	2	1306.89	175

SIIKEPESAAEAVK		28	3	1472.33	364
TLLAQTLAK		28	2	958.75	167
Eukaryotic translation initiation factor 4 gamma 2	**P78344**	**EIF4G2**	**2**	**102**	
Peptide Sequences	Modifications	IonScore	Charge	MH+ [Da]	ΔM [ppm]
TQTPPLGQTPQLGLK		68	2	1578.97	55.6
SYLAQFAAR		59	2	1026.67	133
Estradiol 17-beta-dehydrogenase 8	**Q92506**	**HSD17B8**	**2**	**27**	
Peptide Sequences	Modifications	IonScore	Charge	MH+ [Da]	ΔM [ppm]
SALALVTGAGSGIGR		91	2	1329.87	93.3
AGVIGLTQTAAR		55	2	1157.69	25
signal recognition particle receptor subunit beta	**Q9Y5M8**	**SRPRB**	**5**	**30**	
Peptide Sequences	Modifications	IonScore	Charge	MH+ [Da]	ΔM [ppm]
SAAPSTLDSSSTAPAQLGK		77	2	1788.97	42.1
GDVGSADIQDLEK		63	2	1346.81	126
VADGGGAGGTFQPYLDTLR		53	2	1894.98	33.4
SAAPSTLDSSSTAPAQLGKK		24	3	1916.99	1.62
LQFLER		22	2	805.55	119
Cell cycle and apoptosis regulator protein 2	**Q8N163**	**DBC1**	**6**	**103**	
Peptide Sequences	Modifications	IonScore	Charge	MH+ [Da]	ΔM [ppm]
TLAAEMQELR		56	2	1161.67	68.5
VQTLSNQPLLK		45	2	1240.87	118
FSATEVTNK		34	2	996.65	154
LTPLQLEIQR		28	2	1210.89	147
SPAPPLLHVAALGQK		27	3	1499.03	108
IQVSSEKEAAPDAGAEPITADSDPAYSSK		25	3	2934.28	-30.54
ATP synthase subunit gamma, mitochondrial	**P36542**	**ATP5C1**	**3**	**33**	
Peptide Sequences	Modifications	IonScore	Charge	MH+ [Da]	ΔM [ppm]
IYGLGSLALYEK		51	2	1326.91	138
SEVATLTAAGK		44	2	1047.73	157
HLLIGVSSDR		41	2	1096.61	1.64
Large proline-rich protein BAG6	**P46379**	**BAG6**	**3**	**114**	
Peptide Sequences	Modifications	IonScore	Charge	MH+ [Da]	ΔM [ppm]
AGSSESIAAFIQR		64	2	1336.85	110
LINLVGESLR		36	2	1113.89	207
LQEDPNYSPQRFPNAQR		24	3	2060.17	92.8
Ubiquitin-associated protein 2	**Q5T6F2**	**UBAP2**	**3**	**117**	
Peptide Sequences	Modifications	IonScore	Charge	MH+ [Da]	ΔM [ppm]
DGSLANNPYPGDVTK		63	2	1547.79	38.2
SQPEPSPVLSQLSQR		32	2	1652.93	43.9
AAPLVTSGK		28	2	843.53	46.6
Ran-specific GTPase-activating protein	**P43487**	**RANBP1**	**2**	**23**	
Peptide Sequences	Modifications	IonScore	Charge	MH+ [Da]	ΔM [ppm]
TLEEDEEELFK		55	2	1381.89	185
FASENDLPEWKER		44	3	1621.01	154
Cation-independent mannose-6-phosphate receptor	**P11717**	**IGF2R**	**2**	**266**	
Peptide Sequences	Modifications	IonScore	Charge	MH+ [Da]	ΔM [ppm]
VPIDGPPIDIGR		48	2	1248.91	175
YDLSALVR		37	2	936.75	254
B-cell receptor-associated protein 31	**P51572**	**BCAP31**	**2**	**28**	
Peptide Sequences	Modifications	IonScore	Charge	MH+ [Da]	ΔM [ppm]
LDVGNAEVKLEEENR		59	3	1715.09	137
AENQVLAMR		51	2	1031.67	138
NADH dehydrogenase [ubiquinone] 1 alpha subcomplex subunit 2	**O43678**	**NDUFA2**	**2**	**11**	
Peptide Sequences	Modifications	IonScore	Charge	MH+ [Da]	ΔM [ppm]
ALENVLSGKA		45	2	1001.64	90.1
YAFGQETNVPLNNFSADQVTR		55	3	2371.25	52.4
Inositol-3-phosphate synthase 1	**Q9NPH2**	**ISYNA1**	**3**	**61**	
Peptide Sequences	Modifications	IonScore	Charge	MH+ [Da]	ΔM [ppm]
VGPVAATYPMLNK		50	2	1360.93	150
ADNLIPGSR		27	2	942.71	226
VFVGGDDFK		21	2	983.69	213
EH domain-containing protein 1	**Q9H4M9**	**EHD1**	**3**	**61**	
Peptide Sequences	Modifications	IonScore	Charge	MH+ [Da]	ΔM [ppm]
LLDTVDDmLANDIAR	M8(Oxidation)	61	2	1691.01	107
HLIEQDFPGMR		18	2	1343.29	474
KLNAFGNAFLNR		10	3	1364.51	-167.09
5'-3' exoribonuclease 2	**Q9H0D6**	**XRN2**	**3**	**109**	
Peptide Sequences	Modifications	IonScore	Charge	MH+ [Da]	ΔM [ppm]
NSLGGDVLFVGK		53	2	1205.88	199
GVGAEPLLPWNR		18	2	1308.9	158
AALEEVYPDLTPEETRR		50	3	1989.17	92.1
60S acidic ribosomal protein P1	**P05386**	**RPLP1**	**2**	**12**	
Peptide Sequences	Modifications	IonScore	Charge	MH+ [Da]	ΔM [ppm]

KEESEESDDDMGFGLFD		62	2	1949.9	78.7
AAGVNVEPFWPGLFAK		55	2	1703.03	80.8
NADH dehydrogenase [ubiquinone] 1 beta subcomplex subunit 4	**O95168**	**NDUFB4**	**3**	**15**	
Peptide Sequences	Modifications	IonScore	Charge	MH+ [Da]	ΔM [ppm]
TLPETLDPAEYNISPETR		56	2	2045.96	-14.59
GLIENPALLR		53	2	1095.73	73.7
TINVYPNFRPTPK		20	2	1547.57	476
Conserved oligomeric Golgi complex subunit 5	**Q9UP83**	**COG5,**	**2**	**91**	
Peptide Sequences	Modifications	IonScore	Charge	MH+ [Da]	ΔM [ppm]
NPPSSDELDGIIK		47	2	1384.67	-16.41
STMPTPGNTAALR		19	2	1316.95	220
Protein transport protein Sec24C	**P53992**	**SEC24C**	**3**	**118**	
Peptide Sequences	Modifications	IonScore	Charge	MH+ [Da]	ΔM [ppm]
SPVESTTEPPAVR		45	2	1369.77	56.2
GTEPFVTGVR		22	2	1062.69	127
YASFQVENDQER		11	2	1485.77	75.6
14-3-3 protein theta	**P27348**	**YWHAQ**	**2**	**28**	
Peptide Sequences	Modifications	IonScore	Charge	MH+ [Da]	ΔM [ppm]
qTIDNSQGAYQEAFDISK	N-Term(Gln->pyro-Glu)	71	2	1997.9	2.02
QTIDNSQGAYQEAFDISKK		46	3	2143.09	35.1

Licensed MASCOT software (Matrix Science, UK) was used to unambiguously identify proteins from NCBInr sequence database. NanoLC-MS/MS data were searched using a mass tolerance value of 600 ppm for precursor ion and 0.6 Da for MS/MS fragments, trypsin as the proteolytic enzyme, a missed cleavages maximum value of 1, and Cys carbamidomethylation as fixed modification, and pyroglutamate (peptide N-terminal Gln), pyro-carbamidomethyl Cys (peptide N-terminal CAM-Cys) and Met oxidation as variable modifications. Possible charge states +2 and +3. Candidates with almost 2 assigned peptides with an individual MASCOT score > 44 ($p<0.05$) were considered significant. Protein gene names and UniProt codes were reported as well as the sequence and charge state of each peptide used for identification, the MH+ values, and the error expressed in ppm.

SUPPLEMENTARY TABLE 3. List of ATP7B-H1069Q-specific interactors.

PROTEIN	UNIPROT CODE	GENE NAME	# Peptides	MW [kDa]	
1-phosphatidylinositol 4,5-bisphosphate phosphodiesterase gamma-1	**P19174**	**PLCG1**	**3**	**161**	
Peptide Sequences	Modifications	IonScore	Charge	MH+ [Da]	ΔM [ppm]
SGDITYGQFAQLYR		81	2	1618.87	53.60
TmDLPFLEASTLR	M2(Oxidation)	56	2	1510.01	166.00
APLFPAPK		27	2	840.75	280.00
Golgi apparatus protein 1	**Q92896**	**GLG1**	**2**	**134**	
Peptide Sequences	Modifications	IonScore	Charge	MH+ [Da]	ΔM [ppm]
VAELSSDDFHLDR		59	3	1504.01	205.00
IIIQESALDYR		58	2	1320.91	149.00
Integrin beta-1	**P05556**	**ITGB1**	**4**	**88**	
Peptide Sequences	Modifications	IonScore	Charge	MH+ [Da]	ΔM [ppm]
SAVTTVVNPK		67	2	1015.15	-419.41
IGFGSFVEK		37	2	983.67	156.00
LKPEDITQIQPQQLVLR		31	3	2019.52	186.00
SGEPQTFTLK		19	2	1107.65	76.50
T-complex protein 1 subunit beta	**P78371**	**CCT2**	**8**	**57**	
Peptide Sequences	Modifications	IonScore	Charge	MH+ [Da]	ΔM [ppm]
EALLSSAVDHGSDEVK		70	2	1656.77	-21.01
GATQQILDEAER		61	2	1330.67	9.79
HGINCFINR		48	2	1130.67	107.00
QDLmNIAGTTLSSK	M4(Oxidation)	38	2	1494.89	97.70
VLVDMSR		32	2	819.57	163.00
AAHSEGNTTAGLDMR		15	3	1530.77	51.60
ILIANTGMDTDKIK		44	3	1532.92	65.40
NIGVDNPAAK		21	2	998.63	66.40
60S ribosomal protein L18	**Q07020**	**RPL18**	**5**	**18**	
Peptide Sequences	Modifications	IonScore	Charge	MH+ [Da]	ΔM [ppm]
ILTFDQLALDSPK		58	2	1461.01	187.00
TAVVVGTITDDVR		75	2	1345.89	-14.49
GCGTVLLSGPR		52	2	1116.75	152.00
TNSTFNQVVLK		44	2	1250.73	47.00
SQDIYLR		17	2	894.53	72.50
Proteasome activator complex subunit 1	**Q06323**	**PSME1**	**8**	**28**	
Peptide Sequences	Modifications	IonScore	Charge	MH+ [Da]	ΔM [ppm]
TENLLGSYFPK		61	2	1268.91	206.00
IEDGNNFGVAVQEK		77	2	1519.81	101.00
qLVHELDEAEYR	N-Term(Gln->pyro-Glu)	48	2	1484.83	88.40
APLDIPVPDPVKEK		40	3	1518.47	407.00
LmVMEIR	M2(Oxidation)	39	2	907.67	219.00
IVVLLQR		22	2	840.75	222.00
qPHVGDYR	N-Term(Gln->pyro-Glu)	19	2	954.61	178.00
qLVHELDEAEYRDIR	N-Term(Gln->pyro-Glu)	28	3	1869.28	204.00
CALNEXIN	**P27824**	**CANX**	**7**	**71**	
Peptide Sequences	Modifications	IonScore	Charge	MH+ [Da]	ΔM [ppm]
IVDDWANDGWGLK		77	2	1488.87	108.00
APVPTGEVYFADSFDR		67	2	1770.83	-0.36
GTLSGWILSK		53	2	1061.73	126.00
IVDDWANDGWGLKK		46	3	1617.02	135.00
TPYTImFGPDK	M6(Oxidation)	46	2	1285.77	124.00
LPGDKGLVLmSR	M10(Oxidation)	28	3	1301.87	116.00
IPDPEAVKPDDWDEDAPAK		43	3	2108.02	25.40
Aldehyde dehydrogenase X, mitochondrial	**P30837**	**ALDH1B1**	**4**	**57**	
Peptide Sequences	Modifications	IonScore	Charge	MH+ [Da]	ΔM [ppm]
LAPALATGNTVVMK		63	2	1385.95	123.00
IAKEEIFGPVQPLFK		43	3	1716.35	223.00
VAEQTPLSALYLASLIK		86	2	1817.30	149.00
VTLELGGK		31	2	816.51	37.00
T-complex protein 1 subunit epsilon	**P48643**	**CCT5**	**6**	**59.43073302**	
Peptide Sequences	Modifications	IonScore	Charge	MH+ [Da]	ΔM [ppm]
qQISLATQmVR	N-Term(Gln->pyro-Glu); M9(Oxidation)	78	2	1273.75	75.30
IAILTcPFEPPKPK	C6(Carbamidomethyl)	55	3	1611.47	359.00
GVIVDKDFSHPQmPK	M13(Oxidation)	47	3	1714.85	579.00
TSLGPDGLDK		16	2	1002.54	42.40
LMGLEALK		31	2	874.67	190.00
MLVIEQcK	C7(Carbamidomethyl)	28	2	1020.51	-8.74
40S ribosomal protein S21	**P63220**	**RPS21**	**4**	**8**	
Peptide Sequences	Modifications	IonScore	Charge	MH+ [Da]	ΔM [ppm]
MGESDDSILR		66	2	1122.57	38.50
TYAIcGAIR	C5(Carbamidomethyl)	34	2	1024.53	8.12
RMGESDDSILR		28	2	1278.77	127.00

DHASIQmNVAEVDKVTGR	M7(Oxidation)	50	3	1987	526.00
6-phosphogluconate dehydrogenase, decarboxylating	**P52209**	**PGD**	**6**	**50**	
Peptide Sequences	Modifications	IonScore	Charge	MH+ [Da]	ΔM [ppm]
GILFVGSGVSGGEEGAR		88	2	1591.87	41.00
VDDFLANEAK		53	2	1121.67	112.00
TVSKVDDFLANEAK		44	2	1536.87	53.60
AGQAVDDFIEK		41	2	1192.61	23.70
TIFQGIAAK		28	2	948.67	128.00
SFLEDIRK		17	2	1007.07	-476.16
DNA replication licensing factor MCM3	**P25205**	**MCM3**	**6**	**91**	
Peptide Sequences	Modifications	IonScore	Charge	MH+ [Da]	ΔM [ppm]
TPmENIGLQDSLLSR	M3(Oxidation)	93	2	1689.69	-91.70
GDINILLIGDPSVAK		62	2	1524.31	-361.22
GSSGVGLTAAVTTDQETGER		91	2	1935.92	3.77
VALLDVFR		33	2	932.73	189.00
TLETLIR		33	2	845.69	217.00
LIVNVNDLRR		21	3	1211.9	152.00
40S ribosomal protein S27	**P42677**	**RPS27**	**2**	**10**	
Peptide Sequences	Modifications	IonScore	Charge	MH+ [Da]	ΔM [ppm]
LVQSPNSYFmDVK	M10(Oxidation)	72	2	1543.79	30.20
LTEGcSFR	C5(Carbamidomethyl)	31	2	969.51	69.10
Interleukin enhancer-binding factor 3	**Q12906**	**ILF3**	**7**	**75**	
Peptide Sequences	Modifications	IonScore	Charge	MH+ [Da]	ΔM [ppm]
AYAALAALEK		57	2	1020.69	118.00
EDITQSAQHALR		52	2	1368.57	-83.26
VLQDMGLPTGAEGR		50	2	1443.85	87.80
LFPDTPLALDANK		38	2	1414.77	10.70
VLGMDPLPSK		37	2	1056.75	168.00
LNQLKPGLQYK		27	3	1301.63	160.00
LAAFGQLHK		21	2	984.65	91.70
Peptidyl-prolyl cis-trans isomerase FKBP1A	**P62942**	**FKBP1A**	**3**	**12**	
Peptide Sequences	Modifications	IonScore	Charge	MH+ [Da]	ΔM [ppm]
GVQVETISPGDGR		62	2	1314.75	66.90
GWEEGVAQMSVGQR		57	2	1533.73	13.90
GVQVETISPGDGRTFPK		45	3	1788.11	105.00
Heat shock 70 kDa protein 4L	**O95757**	**HSPA4L**	**2**	**97**	
Peptide Sequences	Modifications	IonScore	Charge	MH+ [Da]	ΔM [ppm]
DISTTLNADEAVAR		85	2	1475.73	-0.60
VLATTFDPYLGGR		64	2	1409.95	149.00
Programmed cell death protein 5	**O14737**	**PDCD5**	**3**	**13**	
Peptide Sequences	Modifications	IonScore	Charge	MH+ [Da]	ΔM [ppm]
NSILAQVLDQSAR		84	2	1414.93	119.00
AVENYLIQmAR	M9(Oxidation)	64	2	1323.43	-181.29
LSNLALVKPEK		18	3	1211.93	165.00
tRNA-splicing ligase RtcB homolog	**Q9Y3I0**	**HSPC117**	**4**	**55**	
Peptide Sequences	Modifications	IonScore	Charge	MH+ [Da]	ΔM [ppm]
qIGNVAALPGIVHR	N-Term(Gln->pyro-Glu)	59	2	1428.01	141.00
SYNDELQFLEK		56	2	1385.79	97.10
IASPEGQDYLK		42	2	1220.79	145.00
SSmTFLTR	M3(Oxidation)	29	2	958.53	69.40
Proteasome activator complex subunit 2	**Q9UL46**	**PSME2**	**5**	**27**	
Peptide Sequences	Modifications	IonScore	Charge	MH+ [Da]	ΔM [ppm]
IEDGNDFGVAIQEK		68	2	1534.89	101.00
ALVHERDEAAYGELR		55	3	1729.01	86.30
TKVEAFQTTISK		33	2	1352.85	81.90
cGFLPGNEK	C1(Carbamidomethyl)	29	2	1021.57	93.70
AmVLDLR	M2(Oxidation)	28	2	833.59	166.00
cytochrome c oxidase subunit 5B, mitochondrial precursor	**Q6FHJ9**	**COX5B**	**3**	**14**	
Peptide Sequences	Modifications	IonScore	Charge	MH+ [Da]	ΔM [ppm]
GLDPYNVLAPK		56	2	1186.69	38.90
KGLDPYNVLAPK		47	3	1315.06	254.00
LVPQQLAH		19	2	905.53	13.70
Cytochrome c oxidase subunit 5A, mitochondrial	**P20674**	**COX5A**	**4**	**17**	
Peptide Sequences	Modifications	IonScore	Charge	MH+ [Da]	ΔM [ppm]
GINTLVTYDmVPEPK	M10(Oxidation)	55	2	1692.91	36.30
LNDFASTVR		47	2	1022.59	64.80
ILEVVKDK		34	2	943.67	96.00
RLNDFASTVR		28	2	1178.85	191.00
Elongation factor 1-beta	**P24534**	**EEF1B2**	**2**	**25**	
Peptide Sequences	Modifications	IonScore	Charge	MH+ [Da]	ΔM [ppm]
SPAGLQVLNDYLADK		88	2	1604.13	187.00
SIQADGLVWGSSK		57	2	1347.77	61.20
ATP synthase subunit e, mitochondrial	**P56385**	**ATP5I**	**3**	**8**	
Peptide Sequences	Modifications	IonScore	Charge	MH+ [Da]	ΔM [ppm]
YSALFLGVAYGATR		45	2	1488.21	-384.33
VPPVQVSPLIK		45	2	1176.81	66.00
ELAEDDSILK		44	2	1132.69	106.00

Thioredoxin domain-containing protein 5	Q8NBS9	TXNDC5	5	44	
Peptide Sequences	Modifications	IonScore	Charge	MH+ [Da]	ΔM [ppm]
GYPTLLWFR		46	2	1152.83	185.00
GYPTLLLFR		45	2	1079.79	156.00
FVLSQAKDEL		39	2	1149.85	207.00
EFPGLAGVK		29	2	917.65	157.00
TLAPTWEELSK		18	2	1274.75	70.70
Dihydrolipoyllysine-residue acetyltransferase component of pyruvate dehydrogenase complex, mitochondrial	P10515	DLAT	3	69	
Peptide Sequences	Modifications	IonScore	Charge	MH+ [Da]	ΔM [ppm]
GVETIANDVVSLATK		99	2	1516.97	99.60
GIDLTQVK		39	2	873.47	-35.86
ILVPEGTR		17	2	884.59	82.30
28S ribosomal protein S28, mitochondrial	Q9Y2Q9	MRPS28	2	20	
Peptide Sequences	Modifications	IonScore	Charge	MH+ [Da]	ΔM [ppm]
NVESFASmLR	M8(Oxidation)	53	2	1169.75	163.00
LLDLELTSR		52	2	1059.832723	216.00
Ubiquitin thioesterase OTUB1	Q96FW1	OTUB1	2	46	
Peptide Sequences	Modifications	IonScore	Charge	MH+ [Da]	ΔM [ppm]
IQQEIAVQNPLVSER		68	2	1723.93	-0.57
LLTSGYLQR		41	2	1050.33	-249.13
EH domain-containing protein 4	Q9H223	EHD4	3	61	
Peptide Sequences	Modifications	IonScore	Charge	MH+ [Da]	ΔM [ppm]
AGGADAVQTVTGGLR		63	2	1372.77	39.90
SISVIDSPGILSGEK		44	2	1502.25	294.00
EYQISAGDFPEVK		30	2	1482.89	123.00
Acetyl-CoA acetyltransferase, cytosolic	Q9BWD1	ACAT2	6	41	
Peptide Sequences	Modifications	IonScore	Charge	MH+ [Da]	ΔM [ppm]
GLIEVKTDEFPR		78	3	1404.02	173.00
VAVLSQNR		40	2	886.79	319.00
ILVTLLHTLER		31	3	1308.14	261.00
VNIEGGAIALGHPLGASGCR		58	3	1949.17	94.1
ELGLNPEK		18	2	899.55	77.30
APHLAYLR		18	2	940.43	-110.22
Fibrinogen gamma chain	P02679	FGG	5	49	
Peptide Sequences	Modifications	IonScore	Charge	MH+ [Da]	ΔM [ppm]
YLQEIYNSNNQK		60	2	1513.95	148.00
TSTADYAmFK	M8(Oxidation)	38	2	1150.57	55.90
qSGLYFIKPLK	N-Term(Gln->pyro-Glu)	30	2	1276.89	128.00
VELEDWNGR		21	2	1117.73	184.00
AIQLTYNPDESSKPNmIDAATLK	M16(Oxidation)	61	3	2536.21	-13.59
Alpha-aminoadipic semialdehyde dehydrogenase	P49419	ALDH7A1	4	54	
Peptide Sequences	Modifications	IonScore	Charge	MH+ [Da]	ΔM [ppm]
VNLLSFTGSTQVGK		59	2	1451.15	250.00
QGLSSSIFTK		46	2	1067.67	93.40
MIGGPILPSER		33	2	1169.79	135.00
VGNPWDPNVLYGPLHTK		40	3	1907.41	233.00
26S proteasome non-ATPase regulatory subunit 2	Q13200	PSMD2	3	94	
Peptide Sequences	Modifications	IonScore	Charge	MH+ [Da]	ΔM [ppm]
VGQAVDVVGQAGKPK		57	3	1453.06	178.00
ELDIMEPKVPDDIYK		34	3	1805.2	173.00
mLVTFDEELRPLPVSVR	M1(Oxidation)	58	3	2018.26	2.37
26S proteasome non-ATPase regulatory subunit 7	P51665	PSMD7	2	28	
Peptide Sequences	Modifications	IonScore	Charge	MH+ [Da]	ΔM [ppm]
DIKDTTVGTLSQR		63	2	1433.75	-4.70
SVVALHNLINNK		57	2	1321.87	86.40
E3 UFM1-protein ligase 1 [Homo sapiens]	O94874	UFL1	5	89	
Peptide Sequences	Modifications	IonScore	Charge	MH+ [Da]	ΔM [ppm]
FFADDTQAALTK		49	2	1327.17	-361.92
AVFVPDIYSR		32	2	1166.77	131.00
SVFMSSTTSASGTGR		31	2	1475.73	36.10
LAADFQR		22	2	820.47	50.70
TYLEVVR		17	2	879.69	227.00
Protein transport protein Sec61 subunit beta	P60468	SEC61B	2	10	
Peptide Sequences	Modifications	IonScore	Charge	MH+ [Da]	ΔM [ppm]
TTSAGTGGMWR		49	2	1124.49	-20.12
FYTEDSPGLK		33	2	1156.65	17.90
26S proteasome non-ATPase regulatory subunit 13	Q9UNM6	PSMD13	5	35	
Peptide Sequences	Modifications	IonScore	Charge	MH+ [Da]	ΔM [ppm]
VLDLQQIK		48	2	956.67	99.70
LNIGDLQVTK		44	2	1100.69	56.10
QLTFEEIAK		40	2	1078.79	199.00
QmTDPNVALTFLEK	M2(Oxidation)	22	2	1623.05	150.00
FLGCVDIKDLPVSEQQER		37	3	2133.37	151.00
Small nuclear ribonucleoprotein E	P62304	SNRPE	3	11	
Peptide Sequences	Modifications	IonScore	Charge	MH+ [Da]	ΔM [ppm]

VmVQPINLIFR	M2(Oxidation)	53	2	1345.89	94.20
ImLKGDNITLLQSVSN	M2(Oxidation)	38	2	1761.95	6.38
GDNITLLQSVSN		33	2	1260.79	119.00
Nuclear migration protein nudC	**Q9Y266**	**NUDC**	**2**	**38**	
Peptide Sequences	Modifications	IonScore	Charge	MH+ [Da]	ΔM [ppm]
GQPAIIDGELYNEVK		54	2	1645.81	-18.50
LVSSDPEINTK		45	2	1202.75	105.00
Ubiquitin carboxyl-terminal hydrolase isozyme L3	**P15374**	**UCHL3**	**2**	**22**	
Peptide Sequences	Modifications	IonScore	Charge	MH+ [Da]	ΔM [ppm]
FLEESVSMSPEER		52	2	1539.69	-4.42
YLENYDAIR		47	2	1156.79	199.00
Ubiquitin conjugation factor E4 A	**Q14139**	**UBE4A**	**2**	**120**	
Peptide Sequences	Modifications	IonScore	Charge	MH+ [Da]	ΔM [ppm]
SYSPTLFAQTVR		58	2	1369.85	104.00
VFVEYIQPK		37	2	1122.87	226.00
Lymphokine-activated killer T-cell-originated protein kinase	**Q96KB5**	**PBK**	**2**	**36**	
Peptide Sequences	Modifications	IonScore	Charge	MH+ [Da]	ΔM [ppm]
ASQDPFPAAIILK		57	2	1370.91	106.00
SLNDLIEER		44	2	1088.65	86.90
Cystatin-B	**P04080**	**CSTB**	**2**	**11**	
Peptide Sequences	Modifications	IonScore	Charge	MH+ [Da]	ΔM [ppm]
SQVVAGTNYFIK		60	2	1326.83	96.20
AKHDELTYF		21	2	1123.65	98.80
Mitogen-activated protein kinase 14	**Q16539**	**MAPK14**	**2**	**41**	
Peptide Sequences	Modifications	IonScore	Charge	MH+ [Da]	ΔM [ppm]
NYIQSLTQmPK	M9(Oxidation)	48	2	1338.53	-104.26
ILDFGLAR		38	2	904.67	163.00
Asparagine--tRNA ligase, cytoplasmic	**O43776**	**NARS**	**3**	**63**	
Peptide Sequences	Modifications	IonScore	Charge	MH+ [Da]	ΔM [ppm]
IFDSEEILAGYKR		45	3	1540.97	114.00
SPAGSIVHELNPNFQPPK		36	3	1931.15	-436.01
IGALEGYR		31	2	878.67	228.00
Dolichyl-diphosphooligosaccharide--protein glycosyltransferase subunit DAD1	**P61803**	**DAD1**	**2**	**12**	
Peptide Sequences	Modifications	IonScore	Charge	MH+ [Da]	ΔM [ppm]
FLEEYLSSTPQR		48	2	1469.79	44.70
SASVVSVISR		28	2	1005.03	458.00
Nucleophosmin	**P06748**	**NPM1**	**2**	**25**	
Peptide Sequences	Modifications	IonScore	Charge	MH+ [Da]	ΔM [ppm]
GPSSVEDIK		47	2	931.55	85.60
LLSISGKR		11	2	873.47	-90.40
6-phosphofructokinase, liver type	**P17858**	**PFKL**	**3**	**90**	
Peptide Sequences	Modifications	IonScore	Charge	MH+ [Da]	ΔM [ppm]
VFANAPDSAcVIGLK	C10(Carbamidomethyl)	45	2	1561.95	95.10
AIGVLTSGGDAQGmNAAVR	M14(Oxidation)	82	2	1803.92	17.20
IMEVIDAITTTAQSHQR		47	3	1914.35	199.00
Acyl-CoA-binding protein	**P07108**	**DBI**	**2**	**10**	
Peptide Sequences	Modifications	IonScore	Charge	MH+ [Da]	ΔM [ppm]
TKPSDEEmLFIYGHYK	M8(Oxidation)	41	3	1973.96	17.30
QATVGDINTERPGMLDFTGK		48	3	2150.24	88.80
S-methyl-5'-thioadenosine phosphorylase	**Q13126**	**MTAP**	**2**	**32**	
Peptide Sequences	Modifications	IonScore	Charge	MH+ [Da]	ΔM [ppm]
YVDTPFGKPSDALILGK		47	3	1821.29	174.00
IGIIGGTGLDDPEILEGRTEK		46	3	2183.39	110.00
Hsp90 co-chaperone Cdc37	**Q16543**	**CDC37**	**3**	**44**	
Peptide Sequences	Modifications	IonScore	Charge	MH+ [Da]	ΔM [ppm]
ASEAKEGEEAGPGDPLLEAVPK		51	3	2195.3	555.00
EGEEAGPGDPLLEAVPK		28	2	1708.04	123.00
LQAEAQQLR		16	2	1056.74	164.00
Alanine aminotransferase 2	**Q8TD30**	**GPT2**	**3**	**58**	
Peptide Sequences	Modifications	IonScore	Charge	MH+ [Da]	ΔM [ppm]
KPFTEVIR		13	2	989.66	96.00
MTILPPVEK		27	2	1027.68	104.00
ANIGDAQAMGQQPITFLR		68	2	1931.04	37.50

Licensed MASCOT software (Matrix Science, UK) was used to unambiguously identify proteins from NCBInr sequence database. NanoLC-MS/MS data were searched using a mass tolerance value of 600 ppm for precursor ion and 0.6 Da for MS/MS fragments, trypsin as the proteolytic enzyme, a missed cleavages maximum value of 1, and Cys carbamidomethylation as fixed modification, and pyroglutamate (peptide N-terminal Gln), pyro-carbamidomethyl Cys (peptide N-terminal CAM-Cys) and Met oxidation as variable modifications. Possible charge states +2 and +3. Candidates with almost 2 assigned peptides with an individual MASCOT score > 44 ($p<0.05$) were considered significant. Protein gene names and UniProt codes were reported as well as the sequence and charge state of each peptide used for identification, the MH+ values, and the error expressed in ppm.

SUPPLEMENTARY MATERIALS AND METHODS

Antibodies, Reagents, DNAs and Adenoviruses

The following antibodies were used. Anti-α-tubulin was from Sigma-Aldrich (St. Louis, USA), anti-TGN46 from AbD Serotec (Oxford, UK), anti-MRP2 from Enzo Life Sciences (Lausen, Switzerland), anti-GM130, anti-giantin and anti-GFP from Abcam (Cambridge, UK), phospho-p38, phospho-JNK, phosphor-ERK, p38, JNK and ERK (Cell Signaling Techology, Beverly MA USA) anti- secondary Alexa Fluor 488, 568, 633, 647-conjugated antibodies were from Invitrogen-Life Technologies (Grand Island, USA), secondary peroxidase conjugate antibodies were from Calbiochem (Darmstadt, Germany). GoldEnhance™ EM kit and 1.4nm gold-conjugated Fab' fragment of anti-rabbit IgGs were from Nanoprobes (Yaphank, NY 11980-9710, USA). The DNAs of GFP-tagged ATP7B and ATP7B^{H1069Q} were provided by Svetlana Lutsenko (John Hopkins Medical School, Baltimore, MD, USA) and by Dominik Huster (University of Leipzig, Leipzig, Germany). The cDNAs of transcription-based luciferase reporter (pGL3-E1b-TATA-4MRE) as well as DNAs of ATP7A and its mutants were reported before (13). DNAs of flag-tagged MKK3, 4, 6 and 7 were obtained from Addgene (Cambridge MA, USA). To obtain the R778L, D765N, L776V, A874V and L1083F mutants of ATP7B, the pEGFPC1-ATP7B construct was used as a template, and site-direct mutagenesis was performed according to the manufacturer instructions for site-directed mutagenesis using the QuickChange kit (Stratagene, La Jolla, CA, USA). Recombinant adenoviruses containing ATP7B-GFP or ATP7B^{H1069Q}-GFP were reported before (14).

Cell culture and Treatments

HeLa, HepG2 cells and primary mouse hepatocytes were grown in Dulbecco's Modified Eagle's medium (DMEM) supplemented with FCS 10% (decomplemented for HepG2 cells), L-glutamine and Penicillin/Streptomycin. HeLa, HepG2 cells and primary

hepatocytes were treated with 200 μM Cu-chelating agent BCS overnight or with 100-200 μM $CuSO_4$ in culture medium at 37°C for 2 or 8 h. To inhibit p38 or JNK specific inhibitors SB202190 (Sigma Aldrich, USA) or SP600125 (Sigma Aldrich, USA) were used respectively. To inhibit protein biosynthesis Cycloheximide (Sigma Aldrich, USA) 100 μg/mL was used at 2,4 and 6 hours. To inhibit the proteasome MG132 (Sigma) 20μM for 4 hours was used.

Adenoviral Infection, DNA Transfection, RNA interference, RNA Preparation and Q-PCR

HeLa and HepG2 cells were infected with first generation adenovirus containing ATP7B-GFP or ATP7B^{H1069Q}-GFP respectively with a multiplicity of infection (MOI) of 50 and 200 virus particles per cell respectively. HepG2 or HeLa cells were transiently transfected with jetPEI TM-Hepatocyte or Trans IT LT1 Transfection transfection reagents (Polyplus transfection, New York NY USA) respectively. siRNAs targeting MAPK8, MAPK9, MAPK10, MAPK11, MAPK12, MAPK13, MAPK14, MAP3K11 were purchased from Sigma-Aldrich and transfected using Oligofectamine (Invitrogen, Carlsbad USA). Total RNAs from control cells and silenced HeLa cells were purified with the using QIA shredder and extracted with RNeasy Protect Mini Kit. Total RNA was converted into cDNA with QuantiTect Reverse Transcription kit. Q-PCR experiments were performed using Light Cycler 480 Syber Green MasterMix for cDNA amplification and in LightCycler 480 II for signal detection. Q-PCR results were analyzed using the comparative Ct method normalized against housekeeping gene β-Actin.

VSVG trafficking assay.

To evaluate the impact of p38 and JNK inhibitors on overall membrane trafficking thermo-sensitive form of vesicular stomatitis virus glycoprotein fused with GFP (VSVG-GFP) was transfected into HeLa cells. Control and inhibitor-treated cells were incubated at 40°C to accumulate VSVG in the ER. Then the temperature was shifted to 32°C to activate VSVG-GFP trafficking. Cells were fixed at different time intervals after the temperature shift and analyzed using confocal microscopy.

Immunofluorescence

Cells were fixed for 10 min with 4% paraformaldehyde (PFA) in 0.2 M HEPES followed by incubation with blocking/permeabilizing solution: 0.5% bovine serum albumin (BSA), 0.1% saponin, 50 mM NH_4Cl in PBS for 20-30 min. Primary and secondary antibodies were diluted in blocking/permeabilizing solution and added to the cells for 1h/overnight or 45 min respectively. Samples were examined with a ZEISS LSM 700 or LSM 710 confocal microscopes equipped with a 63X 1.4 NA oil objective.

For fluorescent Cu detection with CS3 cells were incubated with 5 μM CS3 (kindly provided by Christopher Chang, Berkeley USA) for 15 min at 37°C. CS3 was excited with 561 nm laser of LSM710 and its emission was collected from 565 to 650 nm. Co-localization module of ZEISS ZEN 2008 software was used to measure co-localization of ATP7B with different intracellular markers. ATP7B fluorescent signal inside canalicular domains and CS3 cytosolic and canalicular surface signals were measured using ZEISS ZEN 2008 software and reported in arbitrary units (au).

Fluorescent recovery after photobleaching (FRAP)

Time-lapse sequences from control and inhibitor-treated HeLa cells expressing $ATP7B^{H1069Q}$-GFP were taken at ZEISS LSM 700 or LSM 710 confocal stages at 37°C. Digital images were collected at 3-second intervals. Selective photobleaching of GFP in the Golgi regions was carried out using 100 consecutive scans with a 488 nm laser line at full power. Average fluorescence intensities and $t_{1/2}$ of the recovery in the Golgi regions were quantified using FRAP module of ZEISS ZEN 2008 software.

Western blot analysis

Cells were then solubilized in RIPA buffer. The protein concentration in each sample was evaluated using Bradford Protein Assay. Proteins were eluted with SDS sample buffer and analyzed by immunoblot analysis. Antibodies against GFP, tubulin, phospho-p38, phospho-JNK, p38 and JNK were used.

Immunoprecipitation and mass spectrometry analysis

To identify the effects of ATP7B ^{H1069Q} overexpression on the proteome of liver cell line, proteomics analysis was performed. For the analysis of the hepatocytes overexpressing ATP7B^{H1069Q}-GFP or ATP7B^{WT}-GFP, cell lysates were incubated with the anti-GFP antibody. Then protein G sepharose beads (Sigma, St Louis, MO, USA) were added to each specimen and immune complexes were collected by centrifugation. The beads were then washed and immunoprecipitated proteins were eluted. The eluted proteins were precipitated in methanol/chloroform and then separated by SDS-PAGE. The gel was stained with Coomassie blue. Protein bands were excised from the gel, and digested with trypsin. Peptide mixtures extracted from the gel were analyzed by nano-chromatography tandem mass spectrometry (nanoLC–MS/MS) on a CHIP MS Ion Trap XCT Ultra equipped with a capillary 1100 HPLC system and a chip cube (Agilent Technologies, Palo Alto, CA). Peptide analysis was performed using data-dependent acquisition of one MS scan (mass range from 400 to 2000 m/z) followed by MS/MS scans of the three most abundant ions in each MS scan. Raw data from nanoLC–MS/MS analyses were employed to query a nonredundant protein database using in house MASCOT software (Matrix Science, Boston, USA).

Subcellular fractionation

To determine the amount of ATP7B protein in in different cellular compartments HepG2 expressing ATP7B^{WT}-GFP or ATP7B^{H1069Q}-GFP (control and treated with p38 or JNK inhibitors) were subjected to subcellular fractionation as described in Balch et al (1984). Cells homogenates were separated using discontinuous sucrose density gradient centrifugation. Fractions were collected at in 1.5 ml tubes by aspiration from the bottom, through a capillary tube attached to a polyethylene tube connected to a peristaltic pump and a fraction collector (total of 14 fractions – ~850 µl each). GM130 was used as marker of the Golgi, PDI of the ER and Sodium/Potassium ATPase of plasma membrane. Amonts of GM130, PDI, Na/K-ATPase and ATP7B were revealed in each fractions by Western blot. Briefly, 90 µl of each fraction was mixed with reducing buffer and boiled for 5 min. Samples were loaded in 10% BIS-TRIS gels and run under denaturing conditions. Gels were transferred to nitrocellulose membranes blocked with 1% BSA and

icubated with antibodies against GM130, GFP, PDI or Na/K-ATPase. Anti-rabbit and anti-mouse HRP-conjugated antibodies were used to reveal primary antibodies.

Copper detection by Inductively Coupled Plasma-Mass Spectrometry (ICP-MS)

To determine intracellular Cu concentrations, cell pellets were lysed. The protein concentration in each sample was evaluated using Bradford Protein Assay (BioRad, Segrate, Italy). Cu concentration in the cell lysates was analyzed by ICP-MS. An aliquot of each sample was diluted 1:10 v/v with 5% HNO_3 and analyzed with an Agilent 7700 ICP-MS (Agilent Technologies, Santa Clara, CA, USA) All values of Cu concentration were normalized for protein content in corresponding cell lysates.

Microarray Analysis

To identify the effects of $ATP7B^{H1069Q}$ expression on the transcriptome, total RNA was extracted from HepG2 cells (expressing either $ATP7B^{H1069Q}$-GFP or $ATP7B^{WT}$-GFP) and hybridized on Affymetrix GeneChips. All of the raw microarray data was formatted for 'Gene Expression Omnibus' (GEO) (http://www.ncbi.mln.nih.gov/geo) to comply with Minimum Information About a Microarray Experiment (MIAME) and Microarray Gene Expression Database (MGED) group standards (GEO number GSE51818). The genes differentially expressed in $ATP7B^{H1069Q}$ expressing cells are listed in Supplementary Table 1. Microarray analyses were carried out with R, a free software environment (available at http://www.r-project.org). After quantification of gene expression with robust multi-array normalization (using the BioConductor package affy http://www.bioconductor.org) the significance of the differential gene expression was determined by computing moderated t-statistic s and false discovery rates with the Limma package. Annotation was based on the genome version from the National Center for Biotechnology Information. The p values obtained were corrected for multiple testing by calculating the estimated false discovery rates using the method of Benjamini-Hochberg. Basal and luminal genes that passed all of the described filtering criteria (including the fold-change cut-off) were entered into the Gene Functional Annotation Tool that is available at the Database for Annotation Visualization and Integrated Discovery (DAVID) website (http://david.abcc.ncifcrf.gov) using their official gene

symbols. The gene ontology options GOTERM_BP_ALL and GOTERM_MF_ALL were selected and a functional annotation chart was generated. A maximum p value of 0.05 was chosen to select only the significant categories.

Luciferase Assay

HeLa cells were plated in a 12-well plate and transfected with pGL3-E1b-TATA-4MRE reporter, empty vector (pEGFP-C1), $ATP7B^{WT}$-GFP or $ATP7B^{H1069Q}$-GFP. After 24 hours, cells were treated with 200 μM $CuSO_4$ for 24 hours. Cells were subsequently harvested in a Passive Lysis Buffer (Promega) according to the manufacturer's instructions. Firefly luciferase and *Renilla* luciferase activities were measured with a Dual-Luciferase® reporter assay system (Promega) on a GloMax® 96 Microplate Luminometer (Promega) according to the manufacturer's instructions. Relative Light Units were calculated by dividing firefly measurements by *Renilla* measurements. All values were normalized to the ATP7B expression levels in the respective specimens and an empty vector was used as a control.

Immuno-electron microscopy.

For pre-embedding immuno-electron cells microscopy were fixed with mixture of 4%PFA and 0.05% glutaraldehyde in 0.2 M HEPES for 15 min and with 4%PFA alone for 30 min, followed by incubation with blocking/permeabilizing solution: 0.5% bovine serum albumin (BSA), 0.1% saponin, 50 mM NH_4Cl in PBS for 20-30 min. Primary anti-GFP antibody and 1.4nm gold-conjugated Fab' fragment of anti-rabbit IgGs were diluted in blocking/permeabilizing solution and added to the cells overnight or for 2h respectively. GoldEnhance™ EM kit was used to enhance ultrasmall gold particles. Then cells were scraped, pelleted, post-fixed in OsO_4 and uranyl acetate and embedded in Epon. For cryo immuno-electron microscopy HepG2 cells or small 1 mm^3 pieces of liver tissue from sacrificed mice were rapidly washed in PBS 1X and fixed immediately with a mixture of 2% freshly prepared paraformaldehyde and 0.2% glutaraldehyde in 0.1 M phosphate buffer for 2 h at room temperature. Before freezing in liquid nitrogen cell and tissue gelatin blocks were immersed in 2.3 M sucrose. From each sample, thin plastic or cryo sections were cut using Leica EM UC7 or Leica EM FC7 ultramicrotomes

respectively (Leica Mycrosystems, Vienna, Austria). Cryo sections were double labeled with antibodies against LAMP1 and GFP. EM images were acquired from thin sections using a FEI Tecnai-12 electron microscope (FEI, Eindhoven, Netherlands) equipped with a VELETTA CCD digital camera (Soft Imaging Systems GmbH, Munster, Germany). Morphometric analysis of lysosomal size, distance between lysosomes and PM, distribution of ATP7B among different intacellular compartments was performed using iTEM software (Olympus SYS, Germany).

Statistical analyses

Data were expressed as mean values ± standard deviation. Statistical significance (t-test) was computed using GraphPad Prism6 software. A p-value <0.05 was considered statistically significant. In all figures * means p-value <0.05, ** p-value <0.01, *** p-value <0.001.